nature
structural &
molecular biology

Structural basis for the control of translation initiation during stress

Antón Vila-Sanjurjo[1–3], Barbara-S Schuwirth[1–3], Cathy W Hau[1,2] & Jamie H D Cate[1,2]

During environmental stress, organisms limit protein synthesis by storing inactive ribosomes that are rapidly reactivated when conditions improve. Here we present structural and biochemical data showing that protein Y, an *Escherichia coli* stress protein, fills the tRNA- and mRNA-binding channel of the small ribosomal subunit to stabilize intact ribosomes. Protein Y inhibits translation initiation during cold shock but not at normal temperatures. Furthermore, protein Y competes with conserved translation initiation factors that, in bacteria, are required for ribosomal subunit dissociation. The mechanism used by protein Y to reduce translation initiation during stress and quickly release ribosomes for renewed translation initiation may therefore occur widely in nature.

All organisms contain stress response systems that allow them to survive rapidly changing environmental conditions. In *Escherichia coli* the stress response protein Yfia, or protein Y (PY), binds to 70S ribosomes (monosomes) during cold shock or in early stationary phase and is quickly released once normal growth conditions are restored[1,2]. PY consists of an N-terminal globular domain of 90 amino acids that adopts a βαββββα topology and a flexible C-terminal tail[3,4]. PY stabilizes monosomes against dissociation *in vitro*[5], and has been proposed to affect translation elongation[1,6]. However, its functional role in stress response remains unclear[1,6].

The ribosome plays a central role in adaptation to environmental stress as a checkpoint for sensing shifts in temperature[7] and nutrient levels[8,9]. Ribosomes in all organisms are composed of a small and a large subunit (30S and 50S, respectively, in bacteria) that cycle through stages of association and dissociation during protein synthesis. PY may function as a translational inhibitor during stress by disrupting this cycle through its stabilization of 70S ribosomes[5]. To determine the role of PY interactions with the ribosome, we examined the structural and biochemical basis for PY function in the stress response. Here we show that PY blocks the peptidyl-tRNA site

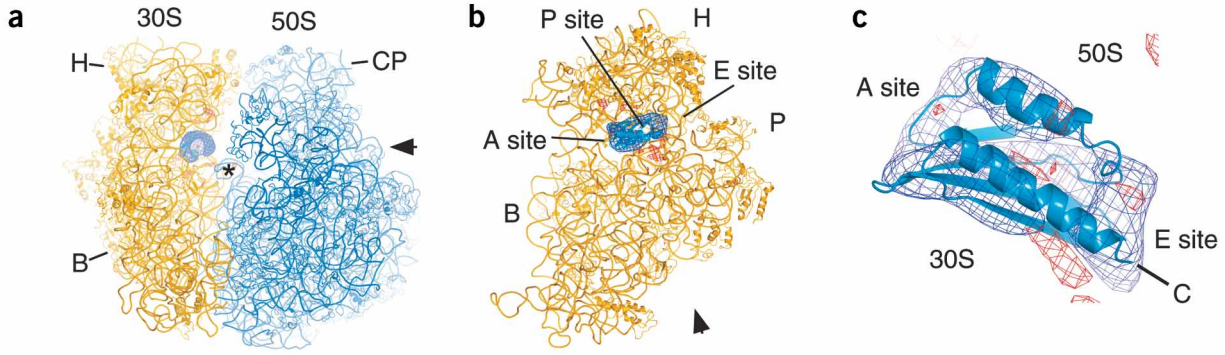

Figure 1 Structural model of protein Y binding to the ribosome as determined by X-ray crystallography. (**a**) Location of PY density in the 70S ribosome. The 30S subunit is gold, the 50S subunit is light blue, positive difference electron density is blue, negative density is red, and PY is cyan. Helix 69 of 23S rRNA is marked with an asterisk. (**b**) PY density in the 30S subunit as seen from the perspective of the subunit interface, indicated by the arrow in **a**. The density occurs between the platform (P) and the head (H) of the 30S subunit. The A, P and E sites, and the body (B) of the small subunit are marked. (**c**) Details of the docking of the N-terminal core of PY (PDB entry 1L4S[3]) into the difference electron density. The position of the disordered C-terminal tail is indicated. The view is from the perspective of the arrow in **b**.

[1]Departments of Molecular and Cell Biology and Chemistry, University of California, Berkeley, California 94720, USA. [2]Lawrence Berkeley National Laboratory, Physical Biosciences Division, Berkeley, California 94720, USA. [3]These authors contributed equally to this work. Correspondence should be addressed to J.H.D.C. (jcate@lbl.gov).

Published online 24 October 2004; doi:10.1038/nsmb850

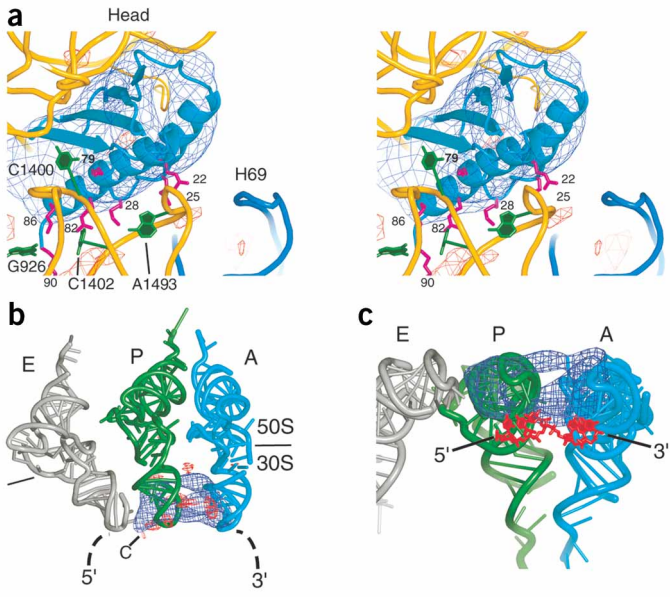

Figure 2 Details of the PY-binding site within the ribosome. (**a**) Stereo view of the location of critical 16S rRNA residues G926, C1400, C1402 and A1493 (green) relative to PY. Helix 69 (H69) of 23S rRNA is blue. Conserved residues within PY are magenta[3]. (**b**) Overlap of PY with A- and P-site tRNAs. A-, P- and E-site tRNAs are cyan, green and gray, respectively. The positions of the 30S and 50S subunits, the path of mRNA, and the location of the C-terminal tail of PY are indicated. (**c**) Overlap of the difference electron density corresponding to PY with mRNA (red). The positive density, E-, A- and P-site tRNAs are color-coded as above. The negative density is not shown for clarity. The 5′ and 3′ ends of the mRNA are marked.

(P site) and aminoacyl-tRNA site (A site) of the ribosome and inhibits translation initiation during cold shock but not under normal growth conditions.

RESULTS

Structure determination

To determine the structural basis for PY stabilization of ribosomes against dissociation into 30S and 50S subunits, we determined the X-ray crystal structure of PY bound to the *E. coli* 70S ribosome. PY was soaked into a new crystal form of the *E. coli* 70S ribosome grown under conditions previously described[10]. Diffraction data were measured to 11.4 Å and 11.0 Å from crystals of 70S ribosomes and 70S ribosomes in a complex with PY, respectively (**Table 1**). The unit cell of the new crystal form is related to the previous form by a five-fold increase in the length of the *c*-axis. On the basis of this relationship, the structure was solved by molecular replacement in which five ribosomes from the small unit cell crystal packing[10] were used as the search model. Crystallographic refinement was carried out as described[10] (**Table 1**).

Position of PY within the ribosome

The X-ray crystal structure reveals that PY binds to the 30S subunit in the 70S ribosome. Difference electron density maps contain features resembling the shape of PY[3,4] near the subunit interface and tRNA-binding sites of all five ribosomes in the crystallographic asymmetric unit (**Fig. 1**). The position of PY supports previous results showing that PY binds to isolated 30S subunits and 70S ribosomes but not to 50S subunits[5]. The only region of the large subunit in close proximity to PY is helix 69 in 23S rRNA, which is ~10 Å from the difference density (**Figs. 1a** and **2a**). Helix 69 plays an essential role both in the association of the two ribosomal subunits and in the transmission of conformational signals between the subunits during elongation[11,12]. However, the structure suggests that PY stabilizes the 70S ribosome without making direct contacts with helix 69 or the large subunit. In agreement with this idea, chemical probing of the large subunit of the ribosome with dimethyl sulfate (DMS) and kethoxal did not reveal any altered reactivity of RNA residues in helix 69 due to the binding of PY (data not shown). Protein Y may therefore stabilize a state of the 30S subunit with high affinity for the 50S subunit, thereby preventing subunit dissociation.

Comparison of PY-, tRNA- and mRNA-binding sites

The difference electron density shows that PY binds across the channel in the 30S subunit where tRNAs and mRNA interact during protein synthesis (**Fig. 1b** and **2**). When superimposed with the positions of tRNAs and mRNA bound to the ribosome in other structures[11,13], PY substantially overlaps the binding sites of both A- and P-site tRNAs but not that of E-site tRNA (**Fig. 2b**). Notably, the conserved positively charged surface in PY[3] lies in close proximity to rRNA residues that are universally conserved markers for the A and P sites[14,15] and that are critical for ribosome function (**Fig. 2a**)[14,16,17]. PY residues Lys86, Lys79 and Arg82 approach the bases of universally conserved residues G926 and C1400 in the P site, and C1402 within a universally conserved wobble pair[17], respectively. PY residues Arg22, Lys25 and Lys28 are near to the backbone of residues that span the P and A sites. Although the present resolution is not sufficient to show that these interactions occur, this possibility is strengthened by results of chemical probing showing that PY binding reduces chemical modification of P-site residues C1400 and G926 (**Fig. 3a**,**b**) and causes enhanced reactivity of A-site residue A1493 (**Fig. 3c**)[14,15]. Enhanced reactivity of A1493 can be explained by the fact that PY binds near the backbone of

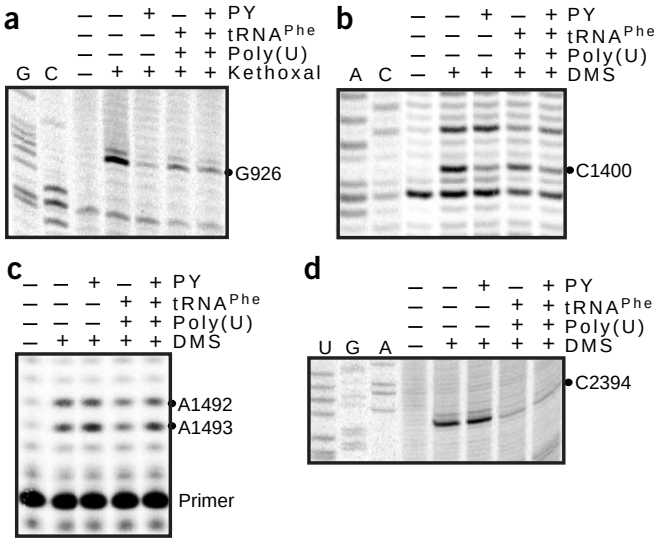

Figure 3 Chemical probing of the ribosome in the presence of PY. (**a**) Kethoxal probing of 16S rRNA in the region of nucleotide 926 (P site). (**b**) Dimethyl sulfate (DMS) probing of the 16S rRNA in the region of nucleotide 1400 (P site). (**c**) DMS probing of the 16S rRNA in the region of nucleotides 1492–1493 (A site). (**d**) DMS probing of the 23S rRNA in the region of nucleotide 2394 (E site). Sequencing lanes are marked by A, C, G or U. Samples are as indicated above each panel.

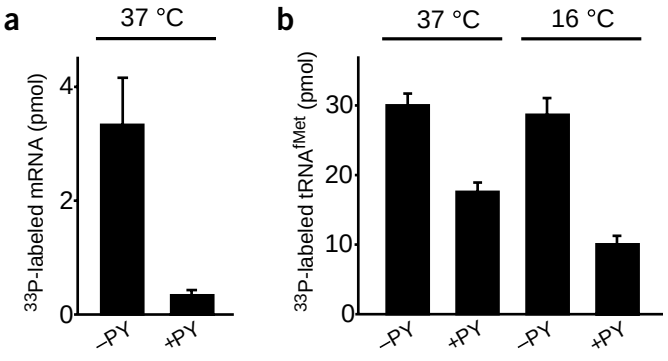

Figure 4 Inhibition of P-site tRNA binding by PY. (**a**) Binding of $tRNA^{fMet}$ to ribosomes programmed with a leaderless mRNA in the presence or absence of PY at 37 °C. The leaderless mRNA was labeled on its 5′ end with [^{33}P]phosphate to follow binding, because leaderless mRNA does not bind to ribosomes in the absence of P-site tRNA (data not shown). (**b**) Experiments were done as in **a** but with an mRNA containing a Shine-Dalgarno sequence. Experiments were carried out at 37 °C or at 16 °C. Average values of three independent experiments with s.d. are shown. $tRNA^{fMet}$ was labeled with [^{33}P]phosphate on its 5′ end to follow binding.

residues 1495–1497 of 16S rRNA and not near the adenine base of A1493 (**Fig. 2a**). Also supporting the structural model, tRNA binds to the E site in the presence of PY, as revealed by the protection of C2394 of 23S rRNA (**Fig. 3d**)[15].

In the structure, the elongated domain of PY only slightly overlaps the position that mRNA would occupy when base-paired with tRNA (**Fig. 2c**). Protection of G926 from chemical probing by the binding of P-site tRNA occurs through contacts to mRNA and not to the tRNA[11,18]. Notably, in the absence of mRNA, the 3′ end of 16S rRNA—a critical element of translation initiation in bacteria[19]—folds back into the mRNA channel of the small subunit[13,18]. Although we cannot determine at the present resolution whether a direct contact between PY and G926 exists, protection of G926 might occur indirectly through the 3′ end of 16S rRNA when no mRNA is present (**Fig. 3a**).

The effect of PY on tRNA binding

PY has been proposed to inhibit protein synthesis during elongation by preventing the binding of A-site tRNA[1]. The structural results above as well as chemical probing experiments support the idea that PY blocks A-site tRNA binding. PY prevents tRNA binding to the A site, as demonstrated by the lack of tRNA-induced protection of A-site residue A1492 and enhancement of A-site residue A1493 (**Fig. 3c**)[15]. However, the above data revealing that PY completely occupies the P site on the 30S subunit suggest that PY primarily functions by preventing P-site tRNA binding, and only indirectly prevents A-site tRNA binding. In filter binding experiments, PY blocks mRNA-dependent P-site tRNA binding in the presence of either a leaderless mRNA (**Fig. 4a**) or an mRNA containing a canonical Shine-Dalgarno (SD) sequence (**Fig. 4b**). Notably, inhibition of P-site tRNA binding by PY in the presence of the SD-containing mRNA is substantially more efficient at 16 °C than at 37 °C (**Fig. 4b**), consistent with a role for PY during cold shock.

The effect of PY on translation initiation

Translational arrest during cold shock has been proposed to occur primarily through an arrest of the initiation of protein synthesis[20]. Translation initiation in bacteria requires the binding of fMet-$tRNA^{fMet}$ to the ribosomal P site in an initiation factor (IF)-dependent reaction[21]. The arrest of translation initiation during cold shock is probably not caused by the cold in itself, as none of the initiation steps, apart from the melting of secondary structures in some mRNAs, is blocked at low temperatures *in vitro*[20]. The position of PY within the ribosomal P site and its ability to prevent P-site tRNA binding suggest that PY may inhibit translation initiation directly, accounting for the observed blocking of initiation at low temperatures. In filter-binding assays, PY competed with the binding of fMet-$tRNA^{fMet}$ to the ribosomal P site in the absence of IFs (**Fig. 5**). However when IFs were present, 70S ribosomes preincubated with PY efficiently bound fMet-$tRNA^{fMet}$ at 37 °C (**Fig. 5a**), indicating that PY does not block initiation under optimal temperature conditions. Notably, PY considerably impaired IF-dependent binding of fMet-$tRNA^{fMet}$ to ribosomes at 16 °C (**Fig. 5b**), consistent with the idea that PY directly arrests initiation during cold shock.

The effect of PY on IF-dependent ribosome dissociation

The above results, together with the fact that translation initiation generally requires the dissociation of the ribosome into the small and large ribosomal subunits, imply that prebound PY would have to be displaced from the P site of the ribosome for initiation to occur. In bacteria, initiation factor 3 (IF3) prevents the 30S subunit from associating with the 50S subunit in early steps of initiation. Because IF3 and PY have opposite effects on ribosome association[5,21], we tested whether IF3 could override PY stabilization of 70S ribosomes. Incubation of 70S ribosomes with PY blocked ribosome dissociation by IF3 (**Fig. 6a**). In the absence of polyamines, IF3 and IF1 worked in tandem to override PY function and dissociate the 70S ribosome (**Fig. 6b**). From the available structural information, it is unclear whether the binding position of PY overlaps with that for IF3[22,23]. However, comparison of the structure of IF1 bound to the 30S subunit[24] with the position of PY in the ribosome shows steric overlap between these two proteins (**Fig. 6c**). This overlap suggests that IF1 directly competes with PY for binding to the 30S subunit.

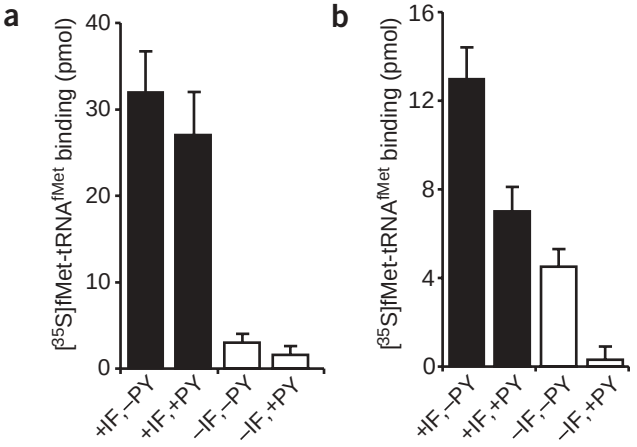

Figure 5 Inhibition of translation initiation by PY. (**a**) Binding of [^{35}S]Met-labeled fMet-$tRNA^{fMet}$ to ribosomes at 37 °C in the absence and presence of PY (–PY and +PY, respectively). Black, IFs were present in reactions (+IF); white, no IFs were present in the reactions (–IF). Average values of four independent experiments with s.d. are shown. (**b**) Reactions were carried out as in **a** but at 16 °C.

DISCUSSION

The results described here provide the first mechanistic view of how *E. coli* controls translation during cold shock. Shortly after cells sense a drop in temperature, the cells enter a period of adaptation to the cold in which translation is arrested by a block in initiation for all but a subset of ~26 cold shock proteins that includes PY[7,20,25]. During cold adaptation, PY binds to the ribosomal P site and effectively blocks most initiation owing to relatively weaker interactions between the ribosome and one or more of the IFs (**Figs. 5** and **6**) and possibly mRNA (**Fig. 4**)[25]. *Cis*-acting elements in cold shock mRNAs or cold shock proteins such as cspA[25] may override PY inhibition of translation to specifically allow expression of cold shock proteins. By blocking the translation of all but cold shock proteins during adaptation, the cell diverts all translation factors to the synthesis of cold shock proteins, thus ensuring its survival in the cold[20]. After cold adaptation, additional ribosomes enter the translating pool[26] and protein synthesis resumes at a much slower rate, as does cell growth[20]. Increased synthesis of IFs during cold shock[20] may help eject PY from some of the inactive monosomes after adaptation. However, a substantial number of ribosomes remain as 70S monosomes[27] stabilized by PY[1,5]. When the optimal growth temperature is restored, PY no longer competes with IFs and quickly dissociates from the ribosome during translation initiation (**Figs. 5** and **6**).

During stress, monosome stabilization by PY[5] serves to protect several conserved elements in the ribosome from degradation: the interface between the ribosomal subunits, key residues lining the A and P sites in the small subunit, and possibly the 3′ end of 16S rRNA. Several lines of evidence suggest that proteins like PY may exist in a large variety of organisms. First, organisms as diverse as bacteria, yeast and mammals form pools of idle monosomes as a general strategy to regulate the translational capacity of the cell during environmental stress[1,2,9,27–30] or limited growth[31]. Second, PY binds to a functionally and structurally conserved region of the ribosome, where it competes with tRNA and highly conserved initiation factors IF1 and IF3. IF1 is universally conserved in structure and function[24,32], and IF3 is functionally analogous to eukaryotic initiation factor 1 (eIF1)[33]. Third, a chloroplast homolog of PY has been shown to bind to the small subunit in chloroplast and *E. coli* monosomes[34,35], suggesting that it also interacts with conserved components of the ribosome. Fourth, in cyanobacteria a homolog of PY is expressed only in the dark, when most protein synthesis is turned off in these bacteria[36], indicating that this protein may act similarly to PY. Proteins with the function of PY may therefore occur widely in nature and serve as rheostats that rapidly tune the level of translation to match environmental conditions.

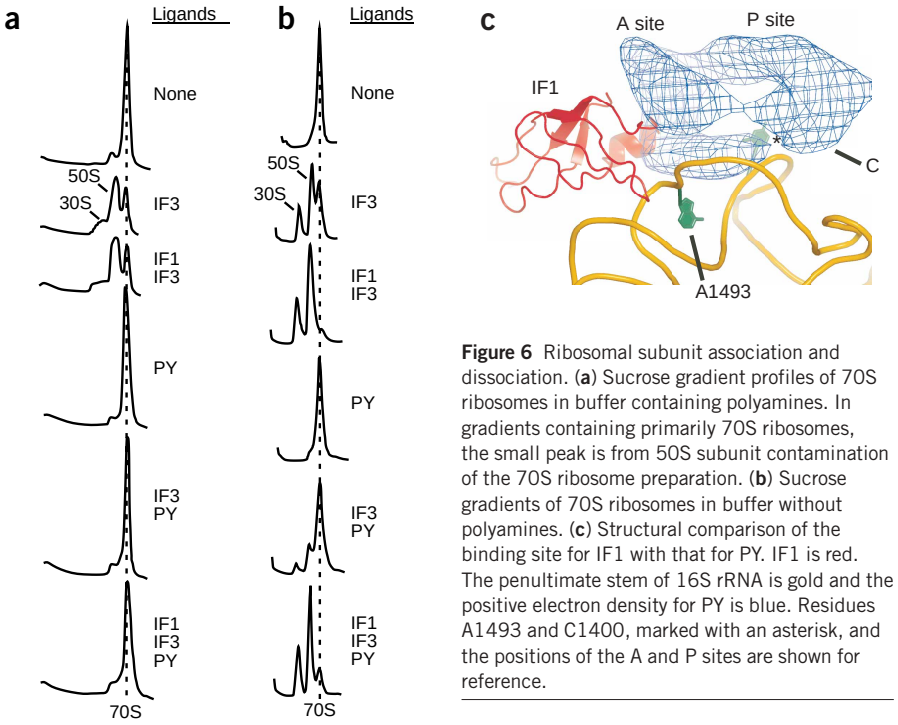

Figure 6 Ribosomal subunit association and dissociation. (**a**) Sucrose gradient profiles of 70S ribosomes in buffer containing polyamines. In gradients containing primarily 70S ribosomes, the small peak is from 50S subunit contamination of the 70S ribosome preparation. (**b**) Sucrose gradients of 70S ribosomes in buffer without polyamines. (**c**) Structural comparison of the binding site for IF1 with that for PY. IF1 is red. The penultimate stem of 16S rRNA is gold and the positive electron density for PY is blue. Residues A1493 and C1400, marked with an asterisk, and the positions of the A and P sites are shown for reference.

Table 1 Diffraction statistics for the *E. coli* 70S ribosome crystals

	Apo 70S	70S–PY complex
Data collection		
Space group	*I*422	*I*422
Cell dimensions		
a, *b*, *c* (Å)	687.9, 687.9, 1933.3	685.8, 685.8, 1928.8
α, β, γ (°)	90, 90, 90	90, 90, 90
Resolution (Å)[a]	500–11.35 (11.8–11.57)	500–10.98 (11.22–10.98)
R_{sym} or R_{merge}[a–c]	18.1 (46.2)	18.9 (47.7)
$I / \sigma I$[a]	7.4 (2.0)	9.2 (2.1)
Completeness (%)[a]	93.9 (77.9)	94.2 (75.6)
Redundancy[a]	6.1 (2.6)	5.5 (3.4)
Refinement[d]		
Resolution (Å)	500–11.5	
No. reflections, R_{work} / R_{free}[e]	62,383 / 6,283	
R_{work} / R_{free}	39.5 / 40.1	
No. atoms	714,210	

[a]Values in parentheses are for the highest-resolution shell. [b]For the apo 70S structure, three crystals were used for data measurement. For the 70S–PY complex, two crystals were used for data measurement. The mean crystal mosaicity for all crystals was 0.3°. [c]Three data measurement passes were used: a high-resolution sweep followed by two low-resolution sweeps. Thus the R_{merge} values in the low-resolution ranges and the overall R_{merge} value of the data are inflated. [d]Refinement involved rigid-body motions only. [e]Amplitudes with $\sigma > 0$.

METHODS

X-ray crystallography. *Escherichia coli* MRE600 streptomycin-dependent 70S ribosomes were purified as described[10]. Protein Y with a C-terminal His-tag was purified by standard nickel-chelate chromatography and dialyzed into storage buffer (20 mM Tris-HCl, pH 7.5, 6 mM $MgCl_2$, 60 mM NH_4Cl, 4 mM 2-mercaptoethanol, 0.5 mM EDTA) containing 10% (v/v) glycerol and stored at –80 °C. The His-tagged version of PY was soaked into a new crystal form of the *E. coli* 70S ribosome grown under conditions described[10]. X-ray diffraction were measured at the Advanced Light Source and reduced as described[10,37]. Because the unit cell of

the new crystal form is related to the previous unit cell by a five-fold increase in the length of the *c*-axis, the structure was solved by molecular replacement in which five ribosomes from the small unit cell crystal packing[10] were used as the search model. The initial molecular replacement model was then refined against structure factor amplitudes measured from crystals of the apo ribosome using rigid body refinement in CNS[38]. An $F_o - F_o$ difference electron density map, calculated using observed structure factor amplitudes and structure factor phases from the molecular replacement model (**Table 1**), was improved by performing real space averaging with RAVE[39]. A truncated model of PY (PDB entry 14LS[3]) lacking the flexible C-terminal tail was docked into the averaged density both manually and with ESSENS[40] with an almost identical outcome. tRNAs and mRNA from the 5.5-Å structure of the 70S ribosome from *Thermus thermophilus* (PDB entry 1GIX[11]), and IF1 in complex with the 30S subunit (PDB entry 1HR0[24]), were superimposed with the structural model of the 70S ribosome–PY complex using O[39]. Figures were created with PyMOL/NUCCYL (DeLano Scientific) and RNAVIEW[41].

Chemical probing. 70S ribosomes (1 μM) were incubated with 4 μM PY or the same volume of PY storage buffer (20 mM Tris, pH 7.5, 6 mM $MgCl_2$, 60 mM NH_4Cl, 4 mM 2-mercaptoethanol, 0.5 mM EDTA) for 15 min at 37 °C, followed by a second incubation in the absence (lanes 1–3) or presence (lanes 4 and 5) of 30 μg ml^{-1} poly(U) mRNA and 7 μM $tRNA^{Phe}$ in 100 μl of probing buffer (25 mM $MgCl_2$, 125 mM NH_4Cl, 80 mM HEPES, pH 7.2) for 15 min at 37 °C. Chemical probing and gel electrophoresis were done as described[10].

Filter binding. Reactions with mRNA containing a Shine-Dalgarno sequence (5′-GUUAACUUUAGU-AGGAGGUAUCAUAUGUUCAAAAAAAAA-3′) were carried out in buffer A containing 50 mM Tris-HCl, pH 7.5, 70 mM NH_4Cl, 30 mM KCl, 7 mM $MgCl_2$ and 1 mM DTT. 70S ribosomes (1 μM) were first incubated with or without 3 μM of PY for 15 min. $tRNA^{fMet}$ (3 μM) labeled on its 5′ end with ^{33}P-phosphate and mRNA containing the Shine-Dalgarno sequence in the ribosome-binding site were added to a final reaction volume of 40 μl and incubated for an additional 15 min. After quenching with 110 μl of reaction buffer, reactions were applied to nitrocellulose filters (Millipore 0.45 μM HA) and washed twice with 1 ml of reaction buffer. Reactions were carried out at either 16 °C or 37 °C. Reactions with leaderless mRNA (5′-pAUGUUC-AAACGUAAUAAU-3′) were carried out in buffer containing 20 mM Tris-HCl, pH 7.5, 60 mM NH_4Cl, 24 mM $MgCl_2$ and 5 mM β-mercaptoethanol. 70S ribosomes (1.9 μM) were incubated with or without 5.7 μM PY at 37 °C for 15 min. The resulting mixtures were then diluted to a final ribosome concentration of 0.25 μM in 10-μl reactions containing 1.5 μM ^{33}P-labeled leaderless mRNA and 1.5 μM deacylated $tRNA^{fMet}$ in the same buffer and incubated for a further 15 min. Reactions were quenched with 300 μl of reaction buffer, applied to nitrocellulose filters as described above, and washed twice with 1 ml of reaction buffer.

Initiation assays. Bulk tRNA enriched in $tRNA^{fMet}$ (15% of the total tRNA) was used to label the initiator tRNA with [^{35}S]Met as described[42]. All reactions were carried out in the presence of polyamines (polymix buffer: 5 mM K-phosphate, pH 7.3, 5 mM $Mg(CH_3COO)_2$, 5 mM NH_4Cl, 95 mM KCl, 0.5 mM $CaCl_2$, 8 mM putrescine, 1 mM spermidine and 1 mM dithioerythritol[43]) as described in the legend to **Figure 5**. 70S ribosomes (1.0 μM) were first incubated with 4 μM PY for 15 min in polymix buffer, followed by the addition of 1.5 μM each of IF1, IF2 and IF3, 3 μM mRNA, 1 mM GTP and 14 μg of [^{35}S]Met-labeled bulk tRNA in a final reaction volume of 40 μl. After a second incubation of 30 min, reactions were quenched with 110 μl of reaction buffer and filtered as described above. Reactions were carried out at either 16 °C or 37 °C.

Separation of ribosomes and ribosomal subunits. 70S ribosomes (1 μM) were first incubated with 3 μM IF3 for 15 min at 37 °C in buffer containing polyamines (20 mM Tris-HCl, pH 7.5, 6 mM $MgCl_2$, 60 mM NH_4Cl, 4 mM 2-mercaptoethanol, 0.5 mM EDTA, 2 mM spermidine and 0.05 mM spermine) or lacking polyamines (50 mM Tris-HCl, pH 7.5, 70 mM NH_4Cl, 30 mM KCl, 7 mM $MgCl_2$ and 1 mM DTT). This was followed by a second incubation with 4 μM PY for 15 min at 37 °C in a final volume of 75 μl. Reactions were layered on 15–40% (w/w) sucrose gradients containing reaction buffer and run for 3 h at 281,000*g* in a Beckmann SW-41 rotor. Experiments with IF3 and IF1 were carried out as above, with the first incubation step containing 3 μM each of IF3 and IF1. The ribosomal subunit composition of each peak in the sucrose gradient was verified by agarose gel electrophoresis (data not shown).

Coordinates. The coordinates and structure factors have been deposited in the Protein Data Bank (accession codes: protein Y-bound 30S, IVOQ, IVOS, IVOV, IVOX and IVOZ; 50S, IVOR, IVOU, IVOW, IVOY and IVP0).

ACKNOWLEDGMENTS

We thank J. Holton, G. Meigs and C. Ralston for help with data measurement at the Advanced Light Source. We thank S. Yang for the PY expression clone, D. Wilson for IF expression clones and K. Nierhaus for the $tRNA^{Phe}$ expression plasmid. We also thank J. Doudna, V. Ramakrishnan, M. O'Connor, M. Marletta and A. Dahlberg and his laboratory for helpful comments on the paper. A.V.-S. acknowledges F. Vila for balance and coherence. This work was funded by the US National Institutes of Health and by the Department of Energy.

COMPETING INTERESTS STATEMENT

The authors declare that they have no competing financial interests.

Received 10 August; accepted 28 September 2004
Published online at http://www.nature.com/nsmb/

1. Agafonov, D.E., Kolb, V.A. & Spirin, A.S. Ribosome-associated protein that inhibits translation at the aminoacyl-tRNA binding stage. *EMBO Rep.* **2**, 399–402 (2001).
2. Maki, Y., Yoshida, H. & Wada, A. Two proteins, YfiA and YhbH, associated with resting ribosomes in stationary phase *Escherichia coli*. *Genes Cells* **5**, 965–974 (2000).
3. Ye, K., Serganov, A., Hu, W., Garber, M. & Patel, D.J. Ribosome-associated factor Y adopts a fold resembling a double-stranded RNA binding domain scaffold. *Eur. J. Biochem.* **269**, 5182–5191 (2002).
4. Rak, A., Kalinin, A., Shcherbakov, D. & Bayer, P. Solution structure of the ribosome-associated cold shock response protein Yfia of *Escherichia coli*. *Biochem. Biophys. Res. Commun.* **299**, 710–714 (2002).
5. Agafonov, D.E., Kolb, V.A., Nazimov, I.V. & Spirin, A.S. A protein residing at the subunit interface of the bacterial ribosome. *Proc. Natl. Acad. Sci. USA* **96**, 12345–12349 (1999).
6. Agafonov, D.E. & Spirin, A.S. The ribosome-associated inhibitor A reduces translation errors. *Biochem. Biophys. Res. Commun.* **320**, 354–358 (2004).
7. VanBogelen, R.A. & Neidhardt, F.C. Ribosomes as sensors of heat and cold shock in *Escherichia coli*. *Proc. Natl. Acad. Sci. USA* **87**, 5589–5593 (1990).
8. Cashel, M., Gentry, D.R., Hernandez, V.J. & Vinella, D. The stringent response. In *Escherichia coli and Salmonella typhimurium: Cellular and Molecular Biology* Vol. 2 (eds. Neidhardt, F.C. *et al.*) 1458–1496 (ASM Press, Washington, DC, 1996).
9. Ashe, M.P., De Long, S.K. & Sachs, A.B. Glucose depletion rapidly inhibits translation initiation in yeast. *Mol. Biol. Cell* **11**, 833–848 (2000).
10. Vila-Sanjurjo, A. *et al.* X-ray crystal structures of the WT and a hyper-accurate ribosome from *Escherichia coli*. *Proc. Natl. Acad. Sci. USA* **100**, 8682–8687 (2003).
11. Yusupov, M.M. *et al.* Crystal structure of the ribosome at 5.5 Å resolution. *Science* **292**, 883–896 (2001).
12. Maivali, U. & Remme, J. Definition of bases in 23S rRNA essential for ribosomal subunit association. *RNA* **10**, 600–604 (2004).
13. Yusupova, G.Z., Yusupov, M.M., Cate, J.H. & Noller, H.F. The path of messenger RNA through the ribosome. *Cell* **106**, 233–241 (2001).
14. Prince, J.B., Taylor, B.H., Thurlow, D.L., Ofengand, J. & Zimmermann, R.A. Covalent crosslinking of tRNA1Val to 16S RNA at the ribosomal P site: identification of crosslinked residues. *Proc. Natl. Acad. Sci. USA* **79**, 5450–5454 (1982).
15. Moazed, D. & Noller, H.F. Intermediate states in the movement of transfer RNA in the ribosome. *Nature* **342**, 142–148 (1989).
16. von Ahsen, U. & Noller, H.F. Identification of bases in 16S rRNA essential for tRNA binding at the 30S ribosomal P site. *Science* **267**, 234–237 (1995).
17. Vila-Sanjurjo, A. & Dahlberg, A.E. Mutational analysis of the conserved bases C1402 and A1500 in the center of the decoding domain of *Escherichia coli* 16 S rRNA reveals an important tertiary interaction. *J. Mol. Biol.* **308**, 457–463 (2001).
18. Wimberly, B.T. *et al.* Structure of the 30S ribosomal subunit. *Nature* **407**, 327–339 (2000).
19. Jacob, W.F., Santer, M. & Dahlberg, A.E. A single base change in the Shine-Dalgarno region of 16S rRNA of *Escherichia coli* affects translation of many proteins. *Proc. Natl. Acad. Sci. USA* **84**, 4757–4761 (1987).
20. Gualerzi, C.O., Giuliodori, A.M. & Pon, C.L. Transcriptional and post-transcriptional control of cold-shock genes. *J. Mol. Biol.* **331**, 527–539 (2003).
21. Brock, S., Szkaradkiewicz, K. & Sprinzl, M. Initiation factors of protein biosynthesis in bacteria and their structural relationship to elongation and termination factors. *Mol. Microbiol.* **29**, 409–417 (1998).
22. McCutcheon, J.P. *et al.* Location of translational initiation factor IF3 on the small ribosomal subunit. *Proc. Natl. Acad. Sci. USA* **96**, 4301–4306 (1999).
23. Dallas, A. & Noller, H.F. Interaction of translation initiation factor 3 with the 30S ribosomal subunit. *Mol. Cell* **8**, 855–864 (2001).
24. Carter, A.P. *et al.* Crystal structure of an initiation factor bound to the 30S ribosomal subunit. *Science* **291**, 498–501 (2001).
25. Giuliodori, A.M., Brandi, A., Gualerzi, C.O. & Pon, C.L. Preferential translation of cold-shock mRNAs during cold adaptation. *RNA* **10**, 265–276 (2004).

26. Thieringer, H.A., Jones, P.G. & Inouye, M. Cold shock and adaptation. *Bioessays* **20**, 49–57 (1998).
27. Uchida, T., Abe, M., Matsuo, K. & Yoneda, M. Amounts of free 70S ribosomes and ribosomal subunits found in *Escherichia coli* at various temperatures. *Biochem. Biophys. Res. Commun.* **41**, 1048–1054 (1970).
28. Broeze, R.J., Solomon, C.J. & Pope, D.H. Effects of low temperature on *in vivo* and *in vitro* protein synthesis in *Escherichia coli* and *Pseudomonas fluorescens*. *J. Bacteriol.* **134**, 861–874 (1978).
29. Barbieri, M., Vittone, A. & Maraldi, N.M. Cell stress and ribosome crystallization. *J. Submicrosc. Cytol. Pathol.* **27**, 199–207 (1995).
30. Ranu, R.S., Levin, D.H., Delaunay, J., Ernst, V. & London, I.M. Regulation of protein synthesis in rabbit reticulocyte lysates: characteristics of inhibition of protein synthesis by a translational inhibitor from heme-deficient lysates and its relationship to the initiation factor which binds Met-tRNAf. *Proc. Natl. Acad. Sci. USA* **73**, 2720–2724 (1976).
31. Cooper, H.L., Berger, S.L. & Braverman, R. Free ribosomes in physiologically nondividing cells. Human peripheral lymphocytes. *J. Biol. Chem.* **251**, 4891–4900 (1976).
32. Kyrpides, N.C. & Woese, C.R. Universally conserved translation initiation factors. *Proc. Natl. Acad. Sci. USA* **95**, 224–228 (1998).
33. Lomakin, I.B., Kolupaeva, V.G., Marintchev, A., Wagner, G. & Pestova, T.V. Position of eukaryotic initiation factor eIF1 on the 40S ribosomal subunit determined by directed hydroxyl radical probing. *Genes Dev.* **17**, 2786–2797 (2003).
34. Johnson, C.H., Kruft, V. & Subramanian, A.R. Identification of a plastid-specific ribosomal protein in the 30S subunit of chloroplast ribosomes and isolation of the cDNA clone encoding its cytoplasmic precursor. *J. Biol. Chem.* **265**, 12790–12795 (1990).
35. Bubunenko, M.G. & Subramanian, A.R. Recognition of novel and divergent higher plant chloroplast ribosomal proteins by *Escherichia coli* ribosome during *in vivo* assembly. *J. Biol. Chem.* **269**, 18223–18231 (1994).
36. Tan, X., Varughese, M. & Widger, W.R. A light-repressed transcript found in *Synechococcus* PCC 7002 is similar to a chloroplast-specific small subunit ribosomal protein and to a transcription modulator protein associated with sigma 54. *J. Biol. Chem.* **269**, 20905–20912 (1994).
37. Otwinowski, Z. & Minor, W. Processing of x-ray diffraction data collected in oscillation mode. *Methods Enzymol.* **276** 307–326 (1997).
38. Brünger, A.T. *et al*. Crystallography & NMR system: A new software suite for macromolecular structure determination. *Acta Crystallogr. D* **54**, 905–921 (1998).
39. Jones, T.A., Zou, J.Y., Cowan, S.W. & Kjeldgaard. Improved methods for building protein models in electron density maps and the location of errors in these models. *Acta Crystallogr. A* **47**, 110–119 (1991).
40. Kleywegt, G.J. & Read, R.J. Not your average density. *Structure* **5**, 1557–1569 (1997).
41. Yang, H. *et al*. Tools for the automatic identification and classification of RNA base pairs. *Nucleic Acids Res.* **31**, 3450–3460 (2003).
42. Ramesh, V., Gite, S., Li, Y. & RajBhandary, U.L. Suppressor mutations in *Escherichia coli* methionyl-tRNA formyltransferase: role of a 16-amino acid insertion module in initiator tRNA recognition. *Proc. Natl. Acad. Sci. USA* **94**, 13524–13529 (1997).
43. Jelenc, P.C. & Kurland, C.G. Nucleoside triphosphate regeneration decreases the frequency of translation errors. *Proc. Natl. Acad. Sci. USA* **76**, 3174–3178 (1979).